# Cesium-induced electronic states and space-charge-layer formation in Cs/InSb(110) interface

Maria Grazia Betti, R. Biagi, U. del Pennino, and Carlo Mariani
*Istituto Nazionale per la Fisica della Materia, Dipartimento di Fisica, Universita' di Modena, Via G. Campi 213/A, 1-41100 Modena, Italy*

M. Pedio
*Istituto di Struttura della Materia–CNR Via Enrico Fermi 38, I-00044 Frascati, Rome, Italy*
(Received 23 October 1995; revised manuscript received 11 January 1996)

We report a study of the electronic properties of Cs overlayers on the narrow-band-gap III-V semiconductor InSb(110) as determined by means of photoemission and high-resolution electron-energy-loss spectroscopy. The electric and electronic properties of Cs-deposited on InSb(110) present *two distinguishable phases*, which can be related to the morphological transition observed in the scanning tunneling microscopy from one-dimensional chains to the two-dimensional (2D) Cs layer. The earlier stages of Cs adsorption induce an accumulation layer, while an additional Cs deposition results in a depletion of carriers in coincidence with the appearance of Cs-induced states in the semiconductor gap. When a 2D layer of cesium is formed on the InSb(110) surface, the interface is *insulating* with the surface band gap at 0.65 eV, larger than the underlying InSb bulk gap (0.175 eV at room temperature).

## I. INTRODUCTION

Alkali metals adsorbed on semiconductor surfaces constitute archetype unreactive systems to explore the mechanism of space-charge-layer formation and the presence of metal-induced states in the semiconductor bulk gap.[1–9] Furthermore, alkali-metal bidimensional layers on semiconductors provide an opportunity to probe the physics of two-dimensional (2D) metal systems, with a simple structure easily accessible for theoretical calculations.[10–12] Current issues subject to active investigation are the charge transfer of the alkali adatoms, the insulator/metal transition in the 2D alkali-adsorbed layers, and the formation of the space-charge layer at the alkali-semiconductor interface.

Among the large amount of experimental and theoretical literature about alkali-metal interaction with semiconductors, the 2D Cs layer deposited on GaAs(110) has been claimed as a prototype of an insulating ordered layer. The atomic structure of the adsorption of cesium on GaAs(110), conceived from scanning tunneling microscopy (STM),[1,2] exhibits three different structural phases. At the earlier coverage stage, one-dimensional (1D) isolated Cs chains form along the [110] direction hundreds of Å apart from each other, providing a model system for testing theories concerning electronic properties of 1D Cs wires. At additional Cs coverages, a 2D overlayer coalesces, and scanning tunneling micrographs show small Cs clusters arranged in a $c(4\times4)$ superlattice.[1,2] Saturating the GaAs(110) surface with additional cesium atoms, a disordered and clustered 3D layer grows.

Our purpose is to extend the study of cesium adsorption to other III-V substrates to test the universality and the driving forces of this interface formation model. We have deposited Cs on the (110) surface of indium antimonide, which has the largest lattice constant of all the zinc-blende III-V semiconductors (15% larger than GaAs). From a scanning tunneling microscopy study,[3,4] the structural phases of Cs adsorbed on InSb(110) are similar to those observed on GaAs(110), but the Cs-Cs bond lengths are larger. In particular, Cs-Cs bonds along the [110] direction lead to Cs-Cs nearest-neighbor distances of 8.0 Å in the 1D Cs chains, and 5.2 Å in a 2D $c(2\times6)$ Cs layer for the Cs/InSb(110) interface [the Cs-Cs distance in bulk Cs is 5.2 Å, and 4.9 Å for the 2D Cs/GaAs(110) interface]. The areal density and the coordination of the Cs atoms are important parameters which drive the dielectric properties (metallic or insulating) of the 2D Cs layer. It is known that liquid Cs undergoes a metal-insulator transition[13] at low density, and that it can be taken as a model for the Mott-Hubbard transition.[14] For this reason the 2D Cs layer on InSb(110) is an appealing candidate for studying this type of Mott insulator.

As far as concerns the insulating properties, from scanning tunneling spectroscopy an opening of the surface gap has been reported in the intermediate stage (2D layer), while, when the 3D system is formed, the Cs/GaAs(110) (Refs. 1 and 2) and Cs/InSb(110) (Refs. 3 and 4) system, exhibit a nearly metallic character. Thus the insulating character of alkali-metal/III-V(110) interfaces seems to be a general characteristic of the 2D Cs overlayer. For the Cs/GaAs(110) interface, an insulator-metal transition has also been observed by direct and inverse photoemission[5] and high-resolution electron-energy-loss spectroscopy.[9] In particular a clear metallic character has been observed for Cs multilayer growth at low temperature.[9]

The aim of this paper is to follow the formation of the 2D Cs layer on InSb(110) from submonolayer coverage to the completion of one monolayer, monitoring either the space-charge-layer formation and the presence of cesium-induced electronic states in the semiconductor gap. Interrelated information on the space-charge layer has been achieved by core-level photoemission and electron energy loss of collective excitations. High-resolution electron-energy-loss spectroscopy (HREELS) is a unique tool, free from radiation-induced effects,[15] for investigating the accumulation (or depletion) layer evolution[16–18] because its probing depth can be tunable

 

on the typical lengths of the space-charge layer. Furthermore, the *extremely high sensitivity* of HREELS to the surface excitations allows us to follow the evolution of Cs-induced electronic transitions in the energy region of the InSb bulk gap. On depositing cesium on InSb(110) the interface appears insulating, with the surface band gap widening at 0.65 eV, confirming previous scanning tunneling spectroscopy (STS) results.[3] At saturation coverage, the nearly metallic character of the Cs/InSb(110) interface has not been observed, in contrast with STS achievements.[3] This experiment delineates the surface sensitivity of the HREELS technique. The metal overlayer deposited on a semiconductor surface shows an opening of a surface gap larger than the bulk band gap of the substrate ($E_g = 0.175$ eV for InSb at room temperature), and in this experimental condition the bulk contribution in the HREEL spectra can be completely neglected.

It is particularly noteworthy to follow concurrently the evolution of the space-charge layer and the band-gap-induced states at the Cs/InSb(110) interface. At very tiny alkali-metal coverages an accumulation layer forms in the same coverage range where 1D Cs chains have been detected; then a reversed band bending and a depletion layer are produced in coincidence with the appearance of the Cs-induced electronic states.

The paper is organized as follows: after an experimental section (II), Sec. III deals with Cs growth morphology, Sec. IV collects the results showing the insulating properties of the Cs overlayer, and Sec. V is devoted to space-charge-layer formation and band bending. The conclusion will be outlined in Sec. VI.

## II. EXPERIMENTAL DETAILS

The high-resolution electron-energy-loss spectroscopy and photoemission experiments were performed in an ultrahigh-vacuum (UHV) system constituted by two chambers, one containing a high-resolution monochromator-analyzer spectrometer (Leybold Heraeus ELS-22), ultraviolet photoemission spectroscopy (UPS) instrumentation and equipped with low-energy electron diffraction (LEED), the other vessel containing all the ancillary equipment for sample cleaning and preparation.

The base pressure in the main chamber was kept below $7\times10^{-11}$ mbar ($7\times10^{-9}$ Pa). The InSb single crystals were $n$-doped ($n = 8.5\times10^{15}$ cm$^{-3}$) bars and the (110) clean surfaces were obtained by cleaving *in situ*. The temperature was monitored with a chromel-alumel thermocouple positioned close to the surface. Cesium was evaporated from well-outgassed dispensers, resistively heated, keeping the base pressure below $1.1\times10^{-10}$ mbar during deposition.

Photoelectron spectra were recorded using a He discharge lamp (He I photons, $h\nu = 21.2$ eV; He II, $h\nu = 40.8$ eV) with a grazing incidence angle. The photoemitted electrons were analyzed with an angle-integrating cylindrical mirror analyzer used at constant energy resolution. The Fermi level was determined on a gold thick layer deposited in electric contact with the sample.

All HREELS measurements were carried out in specular direction geometry with a monochromatic primary beam energy ranging between 3 and 21 eV. The resolution was 8 meV as measured by the full width at half maximum (FWHM) of the elastic peak; it was degraded to about 15 meV in the study of gap region electronic properties, to ensure a good compromise between energy resolution and signal intensity.

The surface cleanness was monitored by checking the absence of the CH and OH stretching frequencies in the HREEL spectra. Extreme care to avoid contamination was taken. The Cs/InSb(110) interface seems very reactive even at liquid-nitrogen temperature, and the presence of cesium suddenly catalyzes the oxidation. After a few hours in ultrahigh vacuum ($10^{-11}$-mbar range), 0.5-ML Cs (or higher coverages) deposited on InSb(110) is highly reactive, and induces additional structures in the photoemission spectra due to the first phase of oxidation: a clear peak at 5.1-eV binding energy appears in the valence-band spectrum, and the Cs $5p$ core levels show a broadening, as already observed in other oxidized alkali-metal/III-V interfaces.[19] For this reason, at coverages higher than 0.5 ML, we have measured every Cs deposition after the cleavage of the clean semiconductor surface in both UP and HREEL spectroscopies.

## III. CESIUM GROWTH ON InSb(110)

### A. Work-function calibration of cesium deposition

As is well known, the deposition of alkali metals on semiconductors and on metals induces a lowering of the ionization energy, i.e., of the work function.[20,21] The calibration of the Cs deposition was performed following a lowering of the work function by measuring the shift of the secondary electron cutoff (sample bias $-10$ V) in ultraviolet photoemission spectra. As in other alkali metals grown on the (110) surface of III-V semiconductors, the variation of the work function with deposition time presents a sudden decrease followed by a minimum value that for the present Cs/InSb(110) experiment is at about 8 min of Cs deposition, as reported in Fig. 1. At saturation, the work function is reduced from the clean surface value by about 3 eV. From the Cs $5p$ core-level intensity we find the saturation coverage at 8 min of Cs deposition time. Thus we assume that 1 ML corresponds to the saturation coverage and it corresponds to about 8 min of Cs deposition. We define 1 ML as an overlayer surface density equal to the substrate surface density, thus as two Cs adatoms per surface unit cell; in the works quoted in Ref. 6, 1 ML is defined as one Cs atom per surface unit cell. We would underline the variety of overlayer coverage definitions; in other works the coverage $\theta = 1$ is considered as the alkali-metal density corresponding to a 2D Cs(110) bcc close-packed layer;[22] therefore the coverage depends on the ratio between the covalent radius of the alkali metal and the substrate lattice parameter. Thus $\theta = 1$ corresponds to 0.75-ML Cs for Cs, InSb(110) and 0.54-ML Cs for Cs/GaAs(110), according to our definition of 1 ML.

### B. Topping model of Cs growth on InSb(110)

Cs growth on InSb(110) at room temperature is characterized by a structural transition from 1D chains to a 2D-layer,[3,4] as previously discussed. Work-function modifications in alkali-metal/semiconductor interfaces are determined by the mutual dipole-dipole interaction as a function

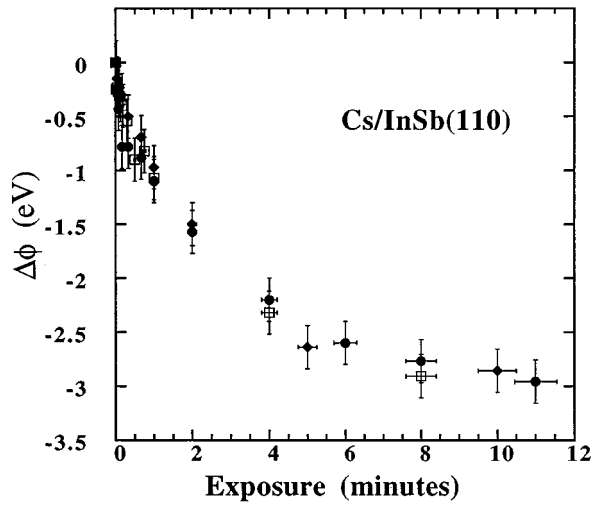


FIG. 1. Work-function change $\Delta\phi$ vs Cs exposure time, as deduced from the cutoff energy for the secondary electrons in the UPS spectra. Different symbols refer to different experimental runs.

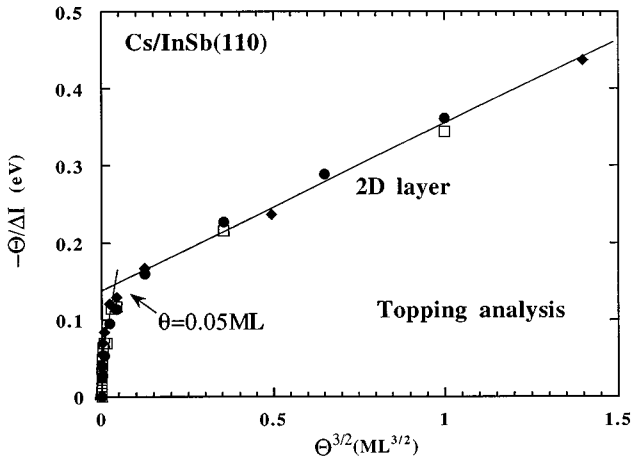


FIG. 2. Plot of $-\Theta/\Delta I$ as a function of $\Theta^{3/2}$ as evaluated from the data shown in Fig. 1. Different symbols refer to different experimental runs. The solid lines represent model fitting to the experimental data, according to the Topping model. Two coverage regions can be singled out, related to different structural phases.

of dipole density per surface unit area; thus information on the growth can be achieved by applying the Topping analysis[23] to the work-function variation at a given adsorbate- (dipole-) substrate system. In particular, a Topping model of the work function has been already used for the Cs/GaAs(110) interface, bringing to light three different adsorption steps at increasing Cs deposition.[20]

The work-function change $\Delta\phi=\Delta I+e_0\Delta V_S$ contains an adsorbate-induced variation of the ionization energy $\Delta I$ and of surface band bending $\Delta V_S$, where $\Delta V_S$ is positive (negative) when the surface bands bend downward (upward). Alkali adatoms on semiconductors establish bond dipoles oriented such as to decrease the ionization energy, and this is the main contribution to the lowering of the work function (see Sec. V). The dipole moment as a function of coverage is given by the Helmholtz equation. On the basis of these assumptions, the expression for the ionization potential is

$$\Delta I=(e/\varepsilon_0)\Theta[p_0/(1+k\alpha_{\mathrm{ad}}\Theta^{3/2})], \tag{1}$$

where $e$ is the electron charge, $\varepsilon_0$ is the vacuum dielectric constant, $\Theta$ is the atomic surface density, $p_0$ is the dipole moment, $\alpha_{\mathrm{ad}}$ is the polarizability of the dipoles, and $k$ a constant determined by the geometry of the adlayer ($k\approx 9$ for square and triangle symmetries of the 2D layer[23]). From this equation the induced dipole moment decreases as a function of coverage and the mutual dipole distances reduce as the number of adatoms per unit area increases. According to the Topping model the curve $-\Theta/\Delta I$ versus $\Theta^{3/2}$ yields a straight line if the geometry of the 2D adlayer preserves the same symmetry ($k$ constant), as has been observed in the case of Cs and K on Si(100),[24] while in other interfaces [Cs/GaAs(110)] straight lines with different slopes have been singled out,[20] indicating different geometrical arrangements.

In Fig. 2 we report the plot of $-\Theta/\Delta I$ versus $\Theta^{3/2}$ for the Cs/InSb(110) interface. The ionization potential has been deduced subtracting the surface band-bending contribution from the work function. However, the band-bending potential makes a minor contribution ($|V_{\mathrm{bb}}|\approx 0.25$ eV) to the whole work-function lowering (about 3 eV), as discussed in Sec. V. As can be noticed from Fig. 2, the plot presents a break point at 0.05 ML. This discontinuity in the Topping model can be ascribed to a morphological transition of the Cs structure and it occurs at the same coverage where STM observes the transition from 1D chains to the 2D layer.[3,4] In the case of Cs adsorption on GaAs(110), Ortega *et al.*[20] report a fitting of the Topping model to the experimental data with two break points, suggesting two structural transitions in agreement with STM results for the Cs/GaAs(110) interface:[1,2] the first break point corresponds to the transition from 1D chains to the 2D structure and the second to the transition from the 2D structure to the 3D compressed layer. The Topping model fitting of our results on the Cs/InSb(110) interface does not exhibit a second structural transition from the 2D region to the 3D compressed layer at 0.5 ML of Cs. This discrepancy between these two Cs/III-V(110) interfaces can be attributed to the lower density of the Cs atoms and to the larger intralayer Cs-Cs bond lengths at the Cs/InSb(110) interface with respect to the Cs/GaAs(110) interface. At the completion of 1 ML of Cs on InSb(110), unlike Cs/GaAs(110), the Cs atoms are not compressed; in fact STM determines the Cs-Cs nearest-neighbor distance at 6.4 Å, while the Cs-Cs distance is 5.2 Å in Cs/GaAs(110).

## IV. IS THE 2D Cs LAYER METALLIC OR INSULATING?

The scattering efficiencies in the energy-loss region of the semiconductor bulk gap in the clean InSb(110) surface and for sequential Cs exposures are collected in Fig. 3. The clean InSb(110) surface exhibits a clear absorption structure with the onset at 175 meV. The main energy-loss feature peaks at 300 meV, representing the maximum of the joint density of states, involving the filled and empty electronic surface states. Angular-resolved photoemission on the InSb(110) clean surface singles out a filled surface state at the $\bar{\Gamma}$ point, resonant with the bulk projected band, that disperses downward to $\bar{X}$ and $\bar{X'}$.[25] This state, labeled $A5$, can be assigned

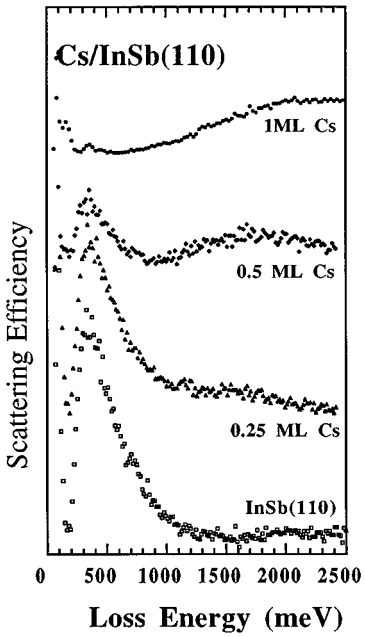


FIG. 3. Scattering efficiency of the Cs/*n*-InSb(110) interface as a function of Cs coverage in the energy region of the InSb semiconductor bulk gap. Primary beam energy $E_p = 15$ eV. Spectra are normalized to the elastic peak height and displaced along the vertical axes for convenience.

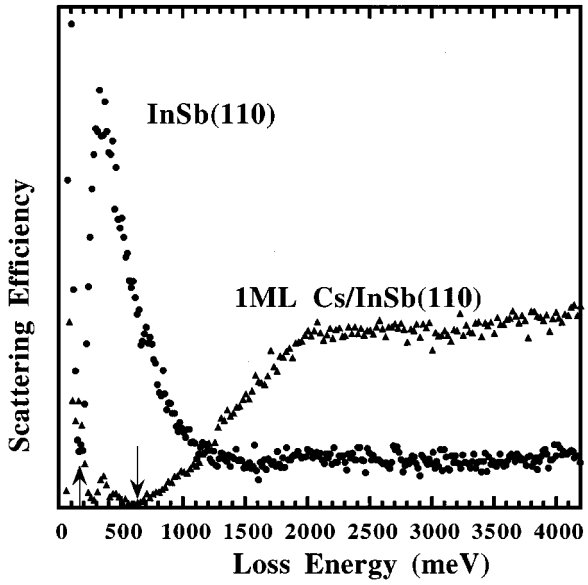


FIG. 4. Scattering efficiency of the clean *n*-InSb(110) and of the 1-ML Cs deposited at room temperature on InSb(110). Primary beam energy $E_p = 15$ eV. Arrows mark the onset energy of the absorption (surface energy gap).

to the initial state of the observed electronic transition at the edge.

On depositing Cs on the InSb(110) surface, we can follow the evolution of the surface gap as reported in Fig. 3. At 0.2 ML a bump appears at high-energy loss, and coexists with the prominent structure at 0.3 eV; when a further amount of Cs is deposited (at 0.5 ML), the surface gap widens and the contribution from the InSb(110) surface states is quenched. For the sake of clarity, we compare the scattering efficiencies of the clean InSb(110) and the 1-ML Cs/InSb(110) in an extended energy-loss range (Fig. 4). At Cs saturation coverage, the surface electronic gap is widened at 0.65 eV, and two broad absorption features are detectable at higher-energy losses. The clear absorption edge at 0.65 eV observed for Cs/InSb(110) seems related to a transition between a filled localized Cs-induced intergap state and the conduction-band minimum. As we will show below, Cs induces a clear structure at 0.45 eV below the Fermi energy in the photoemission spectrum. This state could act as an initial state for the observed electronic transition.

It is noteworthy to emphasize that high-resolution electron-energy-loss spectroscopy is extremely surface sensitive, and that, in a suitable scattering condition such as in this experiment, the bulk contribution in the cross section can be completely neglected. In fact the HREEL spectra after Cs deposition show an opening up of the semiconductor gap, larger than the bulk one.

The elastic peak height, in correspondence to the opening of the gap, is rapidly attenuated, and approaches a value about one order of magnitude lower than on the clean surface. Furthermore, at 1 ML of Cs coverage, the optical active Fuchs-Kliewer (FK) phonon is still present, and its dipole effective charge is not screened by the presence of the alkali-metal overlayer. The persistence of the dipole-active FK phonon and the decrease of the elastic peak intensity are consequences of the insulating character of the interface. A contribution from a disordering of the surface and/or the presence of a clustering of the Cs atoms cannot be excluded. In fact, we observe a diffuse background in the LEED pattern without any evident structural reconstruction, confirming the short-range local order of the structure of the 2D Cs deposited on InSb(110). Thus the $c(2\times6)$ symmetry detected by STM (Refs. 3 and 4) reveals Cs clusters disposed with short-range local order.

From the high-resolution electron-energy-loss spectroscopy results, the insulating character of the 2D Cs layer deposited on the (110) surface of InSb has been clearly observed, confirming STS results. It is well known that bulk metallic cesium is close to the Mott limit,[13,14] and can behave as an insulator. This counterintuitive behavior for the 2D Cs layer, already observed on the Cs/GaAs(110) interface, has been justified with different explanations, all of them based on electron correlation effects.[8–12] In fact, if an odd number of electrons is present in the unit cell and the cation surface states are partially occupied, the interface should be metallic. However, the large Cs-Cs nearest-neighbor distance and the low coordination can induce a localized state and electron-correlation effects. The presence of a correlated electronic system is inappropriate for a one-electron picture, and a Hubbard correlation has been claimed to explain the electronic properties of the 2D insulating alkali layer.[9] Indeed, this model has been proposed to explain the semiconducting behavior of the 2D Cs layer on GaAs(110). The occurrence of the Mott limit can be even more justified for the Cs/InSb(110) interface, where the nearest-neighbor distance for the 2D Cs layer is larger and the areal Cs density on the surface is much lower than on bulk metallic Cs.

As already observed from the Topping model,[23] a clear structural transition on Cs/InSb(110) from the 2D layer to the 3D compressed phase[3,4] has not been observed. Also in the HREEL spectra, we do not distinguish two different behaviors in the dielectric response of the Cs/InSb(110) interface, but only the formation of an insulating interface in the coverage range 0.3–1 ML, due to the highly correlated electronic 2D system that lies below the Mott limit. At saturation coverage, scanning tunneling spectroscopy[3,4] observes a nearly metallic character with a narrowing of the gap below 0.1 eV for Cs/InSb(110) (at the limit of the energy resolution in scanning tunneling spectroscopy[4]) and a metallic behavior for Cs/GaAs(110) interface.[1,2] The narrowing of the band gap has been justified by an increase in Cs density and coordination, reducing the electron correlation and the surface gap value. On the other side, the nearly metallic behavior for both interfaces has not been confirmed by HREELS results.[9] This apparent discrepancy can be ascribed to the local sensitivity of STS spectroscopy, while from the HREELS scattering efficiency the dielectric response is averaged on the whole surface.

Further information on the evolution of the surface electronic structure of cesium deposited on InSb(110) has been achieved by means of photoelectron spectroscopy. The photoemission energy distribution curves in the valence-band (VB) region as a function of sequential Cs deposition at room temperature are collected in Fig. 5.

In the angle-integrated UPS spectra of the clean $n$-type doped InSb(110) surface the valence-band maximum is found 0.2 eV below the Fermi level ($E_F$), indicating flat bands. The first prominent peak at 1.3 eV below $E_F$ is ascribed to the anion dangling-bond states.[25] Several spectral changes are observed as the Cs coverage is increased: the Sb lone pair surface resonance is depressed and a shoulder above the VB maximum (VBM) grows up at 0.25-ML Cs coverage. At about 0.4 ML, a Cs-induced filled state appears at 0.45 eV (labeled $S1$), and the valence-band edge shifts to 0.1 eV below $E_F$ while the anion dangling-bond states are drastically quenched. The saturated 2D Cs overlayer is in a semiconducting state since no photoelectron emission has been detected at the Fermi level, within our experimental uncertainty.

Photoemission experiments have also been performed at low temperature (LT) ($T \approx 120$ K) on LT-deposited Cs layers, in order to investigate whether a multilayer Cs growth and an insulator-metal transition took place. We do not observe significant differences with respect to the room-temperature experiment. The evolution of the Cs-induced states presents the same features, though the Cs-induced filled state appears clearer and better resolved than at room temperature. This spectral analogy indicates that the chemical interaction between the Cs layer and InSb(110) is not substantially modified upon lowering the temperature from 300 to 120 K. Moreover, we observe a saturation of the Cs growth on InSb(110) at low temperature, while a multilayer growth has been achieved on GaAs(110).[6,8,9] It is important to notice that the insulator-metal transition occurs for the Cs/GaAs(110) interface when it undergoes from the 2D layer, with a surface density approximately equal to that of bcc Cs(110), to the 3D film. The absence of an insulator-metal transition in Cs/InSb(110) might be due to a lesser Cs-Cs interaction within the 2D layer caused by the lower Cs areal density on InSb(110) than on GaAs(110).

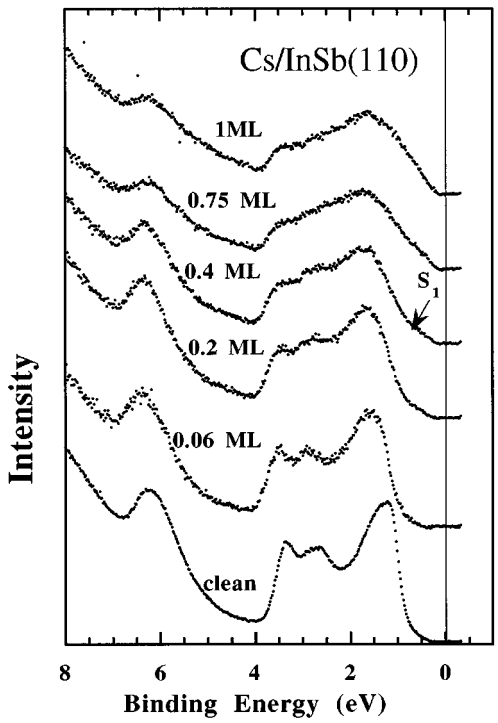


FIG. 5. Angle-integrated UPS spectra in the valence-band region of the clean $n$-type InSb(110) and of the Cs-InSb(110) interface at different Cs exposures. The vertical marks the Fermi energy position. Photon energy of 21.2 eV (He I). Spectra are displaced along the vertical axes for convenience.

The insulating character of the 2D Cs layer grown on InSb(110) has been established by the complementary information inferred from photoemission and HREELS. An open question concerns the dielectric response of Cs/InSb(110) at the very early coverage stage that has been identified below 0.05 ML by Topping analysis, corresponding to a structural phase where 1D Cs chains have been observed by STM.[3,4] At very low Cs coverage (0.04 ML), the HREELS scattering efficiency shows a broadening of the quasielastic peak and the presence of a background underlying the 0.3-eV absorption structure, as reported in Fig. 6. The low-energy tail in the spectrum at 0.04 ML can be interpreted in terms of an increase in the free-carrier concentration contributing to the plasmon losses, as will be discussed in Sec. V. A contribution to the tail from a continuum of intraband transitions in the conduction band cannot be excluded, thus meaning a nearly metallic character of the 1D chains. At the same coverage range, in the valence-band photoemission spectra, emission of electrons from filled states up to $E_F$ has not been detected. The absence of a contribution at the Fermi level can be ascribed to the very low density of $s$-like states present in the valence band. In our opinion, the apparent metallic character of the 1D chains is not due to a proper metallicity of the 1D Cs chains, but mainly derives from the formation of a 2D free-carrier accumulation layer in the InSb conduction band. This behavior will be discussed in detail in Sec. V.

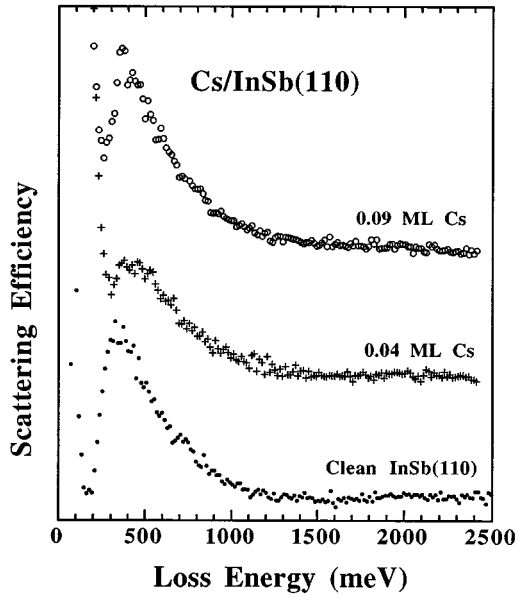


FIG. 6. Selection of HREEL spectra of the Cs/*n*-InSb(110) interface in the energy region of the electronic excitations at very low Cs coverage. Primary beam energy $E_p=15$ eV. Spectra are normalized to the elastic peak height and displaced along the vertical axes for convenience.

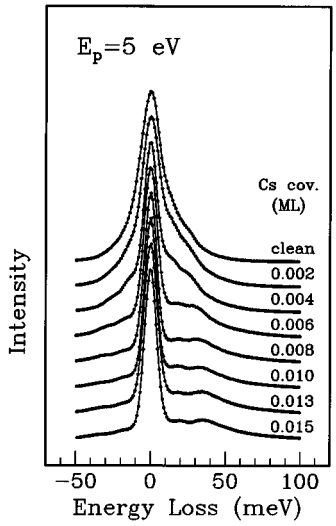


FIG. 7. Selection of HREELS spectra at the Cs/*n*-InSb(110) interface as a function of Cs coverage at the low-coverage stage (0–0.015-ML Cs), in the energy region of the phonon and plasmon losses. Primary beam energy $E_p=5$ eV. Spectra are normalized to the elastic peak height and displaced along the vertical axes for convenience. The phonon and plasmon energies shift to higher-energy losses on increasing Cs coverages. This behavior indicates the formation of an accumulation layer at the interface.

## V. SPACE-CHARGE-LAYER FORMATION AND BAND BENDING

Space-charge-layer formation has been studied through core-level photoemission spectra and collective excitations observed by high-resolution electron-energy-loss spectroscopy. Some significant HREEL spectra, taken in the vibrational loss energy range at different Cs coverage, are reported in Figs. 7 (low Cs coverages, 0–0.015 ML) and 8 (high Cs coverages, 0.03–1 ML).

For the clean nonpolar InSb(110) surface two modes can be clearly resolved; the plasmonlike mode at 15 meV and the phononlike mode at 25 meV. The infrared-active transverse-optical phonon is the Fuchs-Kliewer mode, and the plasmon loss is due to the dopant-induced free-carrier concentration. The plasmon and phonon modes, termed plasmarons,[26] are strongly coupled, and the coupling can determine a dispersion of the two modes.

We first discuss the low-coverage stage (shown in Fig. 7). When as little as 0.002 ML of cesium is deposited, both plasmaron excitations move toward higher energy losses; as the alkali exposure increases the energy-loss shift reaches a maximum above 0.015 ML of coverage. This shift in the energy position and the modification of the intensity of the plasmaron losses are sensitive to the variation of the free-carrier density at the surface. In fact, the plasmon frequency $\omega_p$ is

$$\hbar\omega_p=[(2\pi n_D e^2/m^*\varepsilon_\infty)]^{1/2}, \tag{2}$$

where $n_D$ is the free-carrier density, $m^*$ the effective electron mass, and $\varepsilon_\infty$ the infrared frequency value for InSb dielectric function. If the electron density $n_D$ increases (decreases), as in an accumulation (depletion) layer, the plasmaron losses shift to higher (lower) loss energies. Therefore, the blueshift experienced by the plasmaron modes, in the earlier stage of Cs deposition, is a clear indication of carrier accumulation in the space-charge layer.

The HREEL spectra of the plasmaron modes at higher Cs coverage are collected in Figs. 8(a) and 8(b). As in Fig. 7, the

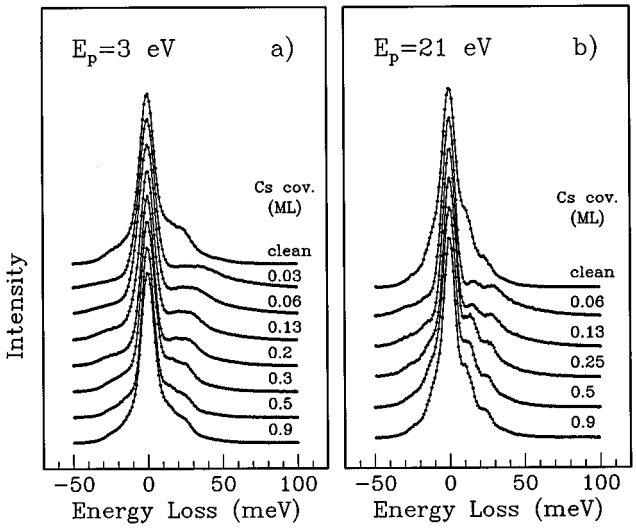


FIG. 8. Selection of HREELS spectra at the Cs/*n*-InSb(110) interface as a function of Cs coverage in the higher-coverage stage (0.03–1-ML, Cs, and clean surface shown for comparison), in the energy region of the phonon and plasmon losses. (a) Primary beam energy $E_p=3$ eV. (b) Primary beam energy $E_p=21$ eV. Spectra are normalized to the elastic peak height and displaced along the vertical axes for convenience. Above 0.03 ML the phonon and plasmon energies shift to lower-energy losses, thus inducating a depletion of carriers at the interface.

maximum energy-loss value of the plasmaron modes occurs at about 0.03-ML Cs. At further Cs deposition, the plasmarons shift to lower energy. At 0.2 ML the data recover the same spectral shape (plasmaron intensity and energy) observed for the clean InSb(110), while at higher Cs coverage a slight redshift suggests the formation of a depletion layer.

This behavior, characterized by two distinct stages in the space-charge-layer configuration, can be confirmed through the analysis of core-level photoemission spectra. The In 4*d* core level of the Cs/*n*-InSb(110) interfaces at selected Cs coverages detected by ultraviolet photoemission spectroscopy are collected in Fig. 9(a). A clear shift to lower kinetic energy is achieved up to a coverage of 0.04 ML, with a subsequent inverse behavior at higher coverages, in strict analogy with what has been observed for the plasmaron losses. At the clean *n*-type doped InSb(110) surface, the Fermi-level position has been measured as coincident with the conduction-band minimum (CBM), within our experimental uncertainty. Thus we can correlate the In 4*d* energy position to the surface Fermi level as a function of Cs coverage, as reported in Fig. 9(b). Since the interface is unreactive and nondisruptive, the In 4*d* core-level energy shifts are related to the surface band bending. When the surface is exposed to an extremely small amount of Cs, the Fermi level enters by 0.25 eV into the conduction band, leading to a band-bending potential $V_{bb} = -0.25$ eV, thus indicating the formation of the accumulation layer. This maximum value of the downward band bending for the accumulation layer occurs at the same Cs coverage for which the highest energy-loss shift of the plasmaron modes is achieved. Further cesium exposures induce an opposite trend: the Fermi level moves back below the conduction-band minimum (at about 0.2-ML Cs) up to a saturation value of 0.15 eV below the CBM, reached at a Cs coverage of 0.6 ML. In this second stage, the space-charge layer is depleted of carriers.

In this section, we have shown that an extremely low amount of cesium deposited on InSb(110) at room temperature induces an electron accumulation layer at the surface. Further deposition of the alkali metal reverses the described behavior up to the formation of a depletion layer. Generally, when a metal is deposited on a narrow-gap semiconductor, the Fermi energy might move inside the conduction band. For example, Cs and Ag deposited on InAs(110) (Refs. 27 and 28) or Ag on InSb(110) (Ref. 29) induce a giant band bending with a Fermi level pinned into the conduction band. A tentative explanation of this inversion can be related to the formation of the Cs-induced filled electronic levels when the structural transition from 1D chains to the 2D layer occur. As can be observed comparing Figs. 7–9 and 2 the inversion of the Fermi-level pinning occurs at the same coverage range where the Topping analysis revealed a transition due to a different interaction between the Cs atoms and the substrate [structural transition from the 1D chains to the 2D layer as observed by STM (Ref. 3)]. Furthermore, the depletion of the carrier concentration starts when Cs-induced filled states appear in the semiconductor bulk gap, as observed by photoemission. These Cs-induced states can behave as a trap for the electron carriers, depleting the accumulation layer at the interface. In conclusion, we have observed that different electrical properties of the Cs/InSb(110) interface and the formation of the space-charge layer can be related to the structural transition from 1D chains to the 2D layer.

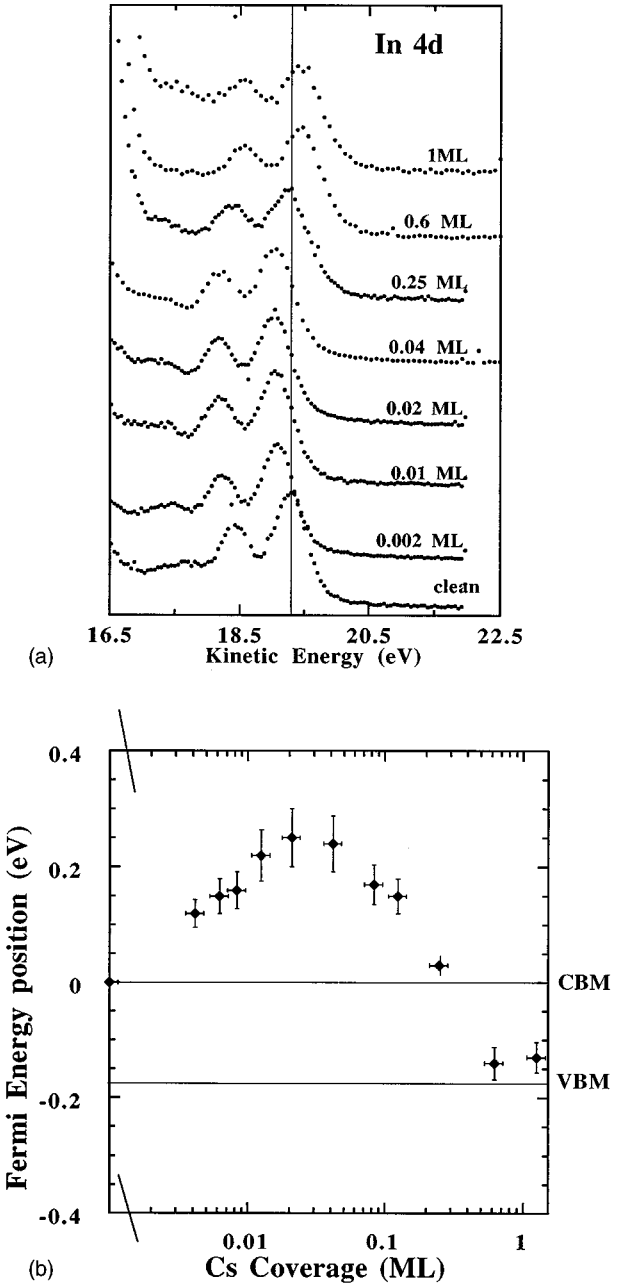


FIG. 9. (a) In 4*d* core-level photoemission spectra as a function of Cs coverage (0–1 ML) and the Cs/*n*-InSb(110) interface, taken at photon energy $h\nu = 40.8$ eV (He II). (b) Surface Fermi-level position with respect to the conduction-band minimum (CBM) at the *n*-InSb(110) surface, as a function of Cs coverage at room temperature. The zero energy line corresponds to the CBM.

## VI. CONCLUSIONS

The electronic and electric properties of the Cs overlayer deposited at room temperature on the InSb(110) present a transition between two discernible phases. This behavior can be related to the structural transition, as observed by STM, from 1D chain formation to the 2D Cs layer.

We have shown that a tiny amount of cesium deposited on InSb(110) at room temperature induces a quantized electron accumulation layer at the surface, and changes drastically the Fermi-level position within the conduction band. When a two-dimensional (2D) layer of cesium is formed, the interface becomes insulating with the surface band gap at 0.65 eV, larger than the InSb bulk gap (0.175 eV at room temperature). The energy value of the 2D Cs/InSb(110) surface gap, similar to that observed on the Cs/GaAs(110) interface at 0.5-ML Cs coverage, seems a property of the 2D Cs layer deposited in III-V(110). In conjunction with photoemission-observations, this is a clear signature that Cs/InSb(110) and Cs/GaAs(110) represent correlated electron systems acting as insulators. The 2D Cs layer on InSb(110) has a lower surface density than on GaAs(110); thus the insulator-metal transition has not been observed at additional Cs deposition on InSb(110), even at low temperature ($T \approx 120$ K).

Furthermore, the 2D Cs layer presents a space-charge layer depleted of carriers. The depletion of the carrier starts when the Cs-induced filled states appear in the semiconductor bulk gap; thus Cs-induced states can act as a trap for the electron carriers.

This is a clear observation, achieved with distinct techniques, of different band-bending mechanisms in a single alkali-metal/semiconductor interface, depending on the structure of the Cs layer (1D chains and 2D layer). This evidence confirms that the Fermi energy position in metal/semiconductor systems is strictly correlated with the atomic structure at the interface.


[1] L. J. Whitman, Joseph Stroscio, R. A. Dragoset, and R. J. Celotta, Phys. Rev. Lett. **66**, 1338 (1991).

[2] P. N. First, R. A. Dragoset, J. A. Stroscio, R. J. Celotta, and R. M. Feenstra, J. Vac. Sci. Technol. A **7**, 2868 (1989).

[3] L. J. Whitman, Joseph Stroscio, R. A. Dragoset, and R. J. Celotta, Phys. Rev. B **44**, 5951 (1991).

[4] L. J. Whitman, Joseph Stroscio, R. A. Dragoset, and R. J. Celotta, J. Vac. Sci. Technol. B **9**, 770 (1991).

[5] K. O. Magnusson and B. Reihl, Phys. Rev. B **40**, 7814 (1989).

[6] T. Maeda Wong, N. J. Di Nardo, D. Heskett, and E. W. Plummer, Phys. Rev. B **41**, 12 342 (1990).

[7] R. Cao, K. Miyano, T. Kendelewicz, I. Lindau, and W. E. Spicer, Phys. Rev. B **39**, 12 655 (1989).

[8] A. B. McLean, D. Heskett, D. Tang, and N. J. DiNardo, Phys. Rev. Lett. **65**, 524 (1990).

[9] N. J. DiNardo, T. Maeda Wong, and E. W. Plummer, Phys. Rev. Lett. **65**, 2177 (1990).

[10] F. Bechstedt and M. Scheffler, Surf. Sci. Rep. **18**, 145 (1993), and references therein.

[11] Z. Gedik, S. Ciraci, and Inder P. Batra, Phys. Rev. B **47**, 16 391 (1993).

[12] J. Hebenstreit, M. Heinemann, and M. Scheffler, Phys. Rev. Lett. **67**, 1031 (1991); Oleg Pankratov and Matthias Scheffler, *ibid.* **71**, 2797 (1993).

[13] A. Ferraz, N. H. March, and F. Flores, J. Phys. Chem. Solids **45**, 627 (1984).

[14] N. F. Mott, Rev. Mod. Phys. **40**, 677 (1968).

[15] M. Alonso, R. Cimino, and K. Horn, Phys. Rev. Lett. **64**, 1947 (1990).

[16] H. Yu and J. C. Hermanson, Phys. Rev. B **40**, 11 851 (1989); **41**, 5991 (1990).

[17] R. Biagi and U. del Pennino, Phys. Rev. B **50**, 7573 (1994).

[18] Maria Grazia Betti, R. Biagi, U. del Pennino, and Carlo Mariani, Europhys. Lett. **32**, 235 (1995).

[19] C. Laubschat, M. Prietsch, M. Domke, E. Wesche, G. Remmers, T. Manel, J. E. Ortega, C. Xue, and G. Kaindl, Phys. Rev. Lett. **62**, 1306 (1989); B. Woratschek, S. Sesselmann, J. Kuppers, and G. Ertl, J. Chem. Phys. **86**, 2411 (1991).

[20] J. E. Ortega and R. Miranda, Appl. Surf. Sci. **56-58**, 211 (1992).

[21] M. Prietsch, C. Laubschat, M. Domke, and G. Kaindl, Europhys. Lett. **6**, 451 (1988).

[22] The surface density of the (110) bcc Cs plane is $3.9\times10^{14}$ cm$^{-2}$ for a metallic radius of Cs, while it is $4.8\times10^{14}$ cm$^{-2}$ for a covalent radius. The surface densities of the (110) surface of GaAs and InSb are $8.85\times10^{14}$ and $6.74\times10^{14}$ cm$^{-2}$, respectively.

[23] J. Topping, Proc. R. Soc. London Ser. A **114**, 67 (1927).

[24] E. M. Oellig and R. Miranda, Surf. Sci. **177**, L947 (1986); J. E. Ortega, E. M. Oellig, J. Feroon, and R. Miranda, Phys. Rev. B **36**, 6213 (1987).

[25] H. U. Middlemann, L. Sorba, V. Hinkel, and K. Horn, Phys. Rev. B **34**, 957 (1986).

[26] J. I. Gersten, Surf. Sci. **92**, 579 (1980).

[27] V. Y. Aristov, G. LeLay, P. Soukiassian, K. Hricovini, J. E. Bonnet, J. Osvald, and O. Olsson, Europhys. Lett. **26**, 359 (1994).

[28] V. Yu. Aristov, G. LeLay, Le Than Vinh, K. Hricovini, and J. E. Bonnet, Phys. Rev. B **47**, 2138 (1993).

[29] V. Yu. Aristov, M. Bertolo, P. Althainz, and K. Jacobi, Surf. Sci. **281**, 74 (1993).